Journal of Computational Methods in Molecular Design, 2014, 4 (2):32-44

Scholars Research Library
(http://scholarsresearchlibrary.com/archive.html)

ISSN : 2231- 3176
CODEN (USA): JCMMDA

A Preliminary Formal Quantitative Structure-Activity Relationship Study of some 1,7-Bis-(amino alkyl)diazachrysene Derivatives as Inhibitors of Botulinum Neurotoxin Serotype A Light Chain and Three *P. falciparum* Malaria Strains.

Juan S. Gómez-Jeria

Quantum Pharmacology Unit, Department of Chemistry, Faculty of Sciences, University of Chile. Las Palmeras 3425, Santiago 7800003, Chile

---

ABSTRACT

Here we present the results of the search for relationships between electronic structure and two biological activities of a group of 1,7-bis-(aminoalkyl)diazachrysene derivatives: the percentages of inhibition of the Botulinum neurotoxin serotype A light chain and the antimalarial activity against three P. falciparum strains. In the case of inhibition of the Botulinum neurotoxin serotype A light chain the results show that the aromatic system is involved in the inhibitory process. There is indirect evidence that one or both side chains could participate in the inhibitory process. In the case of antimalarial activity, the side chains and the aromatic system participate in the process. The antimalarial mechanisms seem to be the same for the three strains. Some suggestions are made to modify these compounds to enhance both activities.

Keywords: QSAR, Botulinum neurotoxin, bioweapons, antimalarial agents, SAR, electronic structure.

INTRODUCTION

Some time ago and regarding structure-activity relationships of cannabinoids, Reggio pointed out that "traditionally, cannabinoid SARs have been focused almost entirely on the independent contribution of certain structural groups ('functional groups') of the molecules *These SARs have been compiled into extensive 'lists of requirements'. This type of approach in SAR studies often assumes the following: that functional groups must react directly with specific sites in the receptor, that modification of one group does not affect the reactivity of another, and that geometric and stereometric factors, such as distance and spatial relationships between functional groups, are all important. Such focus on isolated aspects of the cannabinoids ignores the fact that the molecular properties that are directly responsible for the molecular interactions* (that lead to the pharmacological effect) *are encoded in the entire molecular structure*" (see inside [1]). This statement is still fully valid.

Thus, and from the above perspective, one of the most interesting problems in Quantum Pharmacology is the study of molecules exerting different biological effects on diverse systems. For example, adenofovir dipivoxil acts on the anthrax edema factor and is also employed in chronic hepatitis B viral infection. Another example is miltefosine, used to treat visceral leishmaniasis and breast cancer. The fundamental question to answer is if such different biological activities can be attributed to the same area, to separate areas or to partially overlapping areas of the molecule. When there are enough experimental data measuring the different activities, it is possible to carry out a study to provide information allowing a partial or a full answer to this question.

In this paper we present such an analysis for a group 1,7-bis-(aminoalkyl)diazachrysene derivatives acting as inhibitors of the Botulinum neurotoxin serotype A light chain, three *P. falcifarum* malaria strains and the Ebola filovirus [2]. Malaria and botulism are too well known as health problems to describe them here; therefore we refer the reader to the literature [3-18].

MATERIALS AND METHODS

Methods.

The method employed here has been widely explained, discussed and applied in several papers [19-52]. Here we present a standard summary that has been employed in the same form in other publications [44-52].

It is proposed that the logarithm of any biological activity, BA, can be expressed as the following linear function of several local atomic reactivity indices (LARIs):

$$\log(\mathrm{BA}) = a + \sum_j \left[e_j Q_j + f_j S_j^E + s_j S_j^N \right] +$$
$$+ \sum_j \sum_m \left[h_j(m) F_j(m) + x_j(m) S_j^E(m) \right] + \sum_j \sum_{m'} \left[r_j(m') F_j(m') + t_j(m') S_j^N(m') \right] +$$
$$+ \sum_j \left[g_j \mu_j + k_j \eta_j + o_j \omega_j + z_j \varsigma_j + w_j Q_j^{\max} \right] + \sum_{B=1}^{W} O_B \qquad (1)$$

Table 1 presents, in the standard form used in other publications, the physical interpretation and units of the LARIs, together with references corresponding to their first historical use [40, 53, 54]. The nomenclature employed hereafter is the following. $HOMO_j$* is the highest occupied molecular orbital localized on atom j and $LUMO_j$* is the lowest empty molecular orbital (MO) localized on atom j. They are called the local atomic frontier MOs. The molecular MOs do not carry an asterisk.

Table 1. LARIs and their physical meaning.

LARI	Name	Physical interpretation	Units
Q_i	Net atomic charge of atom i	Electrostatic interaction [53]	e
S_i^E	Total atomic electrophilic superdelocalizability of atom i	Total atomic electron-donating capacity of atom i (MO-MO interaction) [54]	e/eV
S_i^N	Total atomic nucleophilic superdelocalizability of atom i	Total atomic electron-accepting capacity of atom i (MO-MO interaction) [54]	e/eV
$S_i^E(m)$	Orbital atomic electrophilic superdelocalizability of atom i and occupied MO m	Electron-donating capacity of atom i at occupied MO m (MO-MO interaction) [54]	e/eV
$S_i^N(m')$	Orbital atomic nucleophilic superdelocalizability of atom i and empty MO m'	Electron-accepting capacity of atom i at vacant MO m' (MO-MO interaction) [54]	e/eV
F_i	Fukui index of atom i	Total electron population of atom i (MO-MO interaction) [54]	e
F_{mi}	Fukui index of atom i and occupied MO m.	Electron population of occupied m MO at atom i (MO-MO interaction) [54]	e
$F_{m'i}$	Fukui index of atom i and empty MO m'	Electron population of vacant MO m' at atom i (MO-MO interaction) [54]	e
μ_i	Local atomic electronic chemical potential of atom i	Propensity of atom i to gain or lose electrons. $HOMO_i$*-$LUMO_i$* midpoint [40]	eV
η_i	Local atomic hardness of atom i	Resistance of atom i to exchange electrons with the environment [40] $HOMO_i$*-$LUMO_i$* gap	eV
ς_i	Local atomic softness of atom i	The inverse of η_i [40]	1/eV
ω_i	Local atomic electrophilicity of atom i	Tendency of atom i to receive extra electronic charge together with its resistance to exchange charge with the medium	eV
$Q_i^{\max}$	Local atomic charge capacity	Maximal amount of electronic charge atom i may receive [40]	---
O_t	Orientational Parameter of the substituent	A parameter influencing the fraction of molecules attaining the correct orientation to interact with a partner [27, 30]	uma·Å^2

Selection of the experimental data

The biological activities selected for this study are the percentage of inhibition of BoNT/A LC (BO hereafter) calculated at a 20 μM concentration and the *in vitro* antimalarial activity measured for a *P. falciparum* clone of the Sierra I/UNC isolate (D6), a *P. falciparum* clone of the Indochina I isolate (W2) and a *P. falciparum* clone of a

South-East Asian isolate strain (Thailand, C235) [2]. The molecules and their biological activities are displayed in Fig. 1 and Table 2. Cytotoxicity (CT) results were also included in this study. Experimental results concerning the *in vitro* inhibition of Ebola filovirus were not included because of the lack of sufficient experimental data.

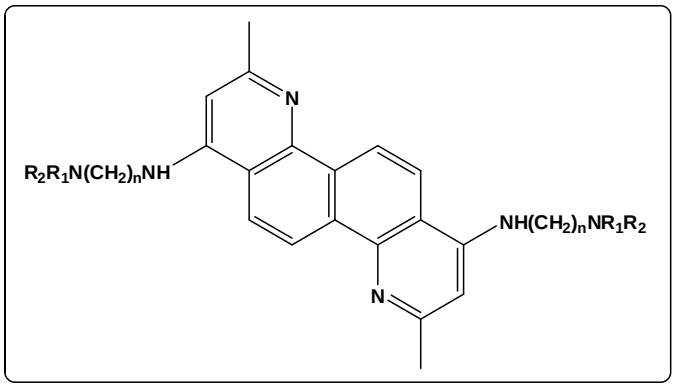

Figure 1. General formula of 1,7-bis-(aminoalkyl)diazachrysene derivatives.

Table 2. Selected molecules and their biological activities.

Mol.	R_1	R_2	n	log(CT)	log(BT)	$\log(IC_{50})$ D6	$\log(IC_{50})$ W2	$\log(IC_{50})$ C235
1	Et	Et	3	3.06	1.81	1.48	0.94	1.82
2	H	H	4	---	1.86	---	---	---
3	H	H	3	3.33	1.85	2.85	3.23	3.31
4	H	H	2	3.72	1.80	2.43	2.94	3.01
5	Me	Me	3	3.00	1.84	2.01	2.55	1.74
6	Me	Me	2	3.41	1.76	1.19	0.96	1.18
7	Et	Et	2	3.97	1.74	0.78	0.54	0.52
8	$-(CH_2)_4-$		3	2.65	1.87	1.17	0.89	1.54
9	$-(CH_2)_4-$		2	3.69	1.78	1.22	0.91	1.41
10	$-(CH_2)_5-$		3	3.17	1.82	0.97	0.84	1.40
11	$-(CH_2)_5-$		2	3.27	1.80	0.94	0.74	1.02
12	$(CH_2CH_2)_2O$		3	3.87	1.75	0.72	0.30	0.91
13	$(CH_2CH_2)_2O$		2	4.01	1.59	0.77	0.79	0.99

Calculations

The electronic structure of the molecules was obtained within the DFT framework at the B3LYP/6-31g(d,p) level with full geometry optimization. It is important to mention that the full geometry optimization was carried out with the option 'ignore symmetry` that may produce local minima. The Gaussian suite of programs was employed [55]. The values of the LARIs were obtained with the D-CENT-QSAR software [56]. Mulliken Population Analysis results were corrected to eliminate negative electron populations and MO populations greater than 2 [57]. Orientational parameters were calculated as usual [27, 30]. Considering that it is not possible to solve the system of linear equations because there are not enough cases (molecules), we employed Linear Multiple Regression Analysis (LMRA) to discover which atoms are implicated in the variation of the BA. We worked with the premise that there is a set of atoms common to all the molecules studied (the common skeleton), encoding the variation of the biological activity throughout the series. Then, it is the variation of the values of some local atomic reactivity indices of some atoms of the common skeleton that accounts for the variation of the inhibition of the BA throughout the series analyzed. The role of the substituents is to modify the electronic structure of the common skeleton and to control the precise alignment of the common skeleton with its partner. For the LMRA, we built separate matrices containing the logarithm of the dependent variable (the selected BA in each case) and the local atomic reactivity indices of the atoms of the common skeleton as independent variables. The Statistica software was used [58]. The common skeleton numbering is shown in Fig. 2. It is important to mention that, as the side chains are of different lengths, we have incorporated into the common skeleton the N-C-C fragment directly attached to the aromatic system plus the nitrogen atom at the end of the chain.

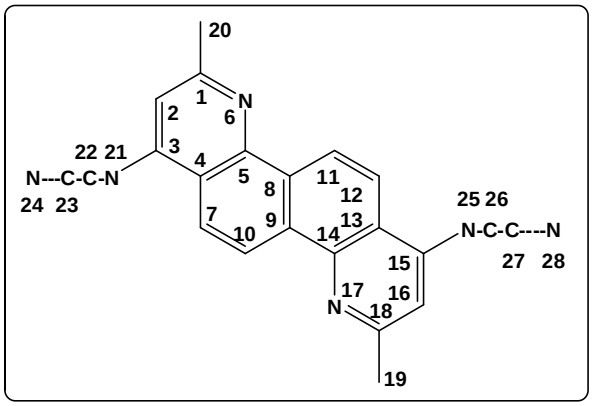

Figure 2. Common skeleton of 1,7-bis-(aminoalkyl)diazachrysene derivatives.

RESULTS

Analysis of the correlation between experimental results.
Table 3 shows the squared correlation coefficients for the experimentally reported values of biological activities.

Table 3: Squared correlation coefficients of the experimental values.

	log(CT)	log(BO)	log(IC_{50}) D6	log(IC_{50}) W2
log(BO)	0.61	1.00		
log(IC_{50}) D6	0.06	0.25	1.00	
log(IC_{50}) W2	0.03	0.16	0.94	1.00
log(IC_{50}) C235	0.06	0.23	0.90	0.81

We can see that there is a high degree of correlation between the log(IC_{50}) values for the three *P. falciparum* strains. Given the similarity of these three biological systems we can expect that, if the mechanism of action is similar, we shall obtain very similar or identical results in the LMRA.

Results for BoNT/A LC inhibition
For the BoNT/a LC % inhibition we obtained the following statistically significant equation:

$$\log(BO) = 5.10 - 15.95F_{15}(LUMO+2)^* - 0.033S_4^N(LUMO+1)^* - 0.85S_{16}^E(HOMO-2)^* \quad (2)$$

with n=12, R=0.98, R^2=0.95, adj R^2=0.94, F(3,9)=62.49 (*p<0.000001*) and SD=0.02. No outliers were detected and no residuals fall outside the ±2.0025σ limits. Here $F_{15}(LUMO+2)^*$ is the Fukui index (electron population) of the third vacant local MO localized on atom 15, $S_4^N(LUMO+1)^*$ is the orbital nucleophilic superdelocalizability of the second vacant local MO localized on atom 4 and $S_{16}^E(HOMO-2)^*$ is the orbital electrophilic superdelocalizability of the third highest occupied MO localized on atom 16. Tables 4 and 5 show, respectively, the beta coefficients, the results of the t-test for significance of coefficients and the matrix of squared correlation coefficients for the variables appearing in Eq. 2. Table 5 shows that there are no significant internal correlations between independent variables. Figure 3 shows the plot of observed *vs.* calculated values. The associated statistical parameters of Eq. 2 show that this equation is statistically significant and that the variation of a group of local atomic reactivity indices belonging to the common skeleton explains about 94% of the variation of the BoNT/A LC inhibition percentage.

Table 4: Beta coefficients and *t*-test for significance of the coefficients in Eq. 2.

	Beta	t(9)	*p-level*
$F_{15}(LUMO+2)^*$	-0.93	-12.42	<0.000001
$S_4^N(LUMO+1)^*$	-0.46	-5.98	<0.0002
$S_{16}^E(HOMO-2)^*$	-0.23	-3.03	<0.014

Table 5: Squared correlation coefficients for the variables appearing in Eq. 2.

	$F_{15}(LUMO+2)^*$	$S_4^N(LUMO+1)^*$
$S_4^N(LUMO+1)^*$	0.05	1.00
$S_{16}^E(HOMO-2)^*$	0.05	0.10

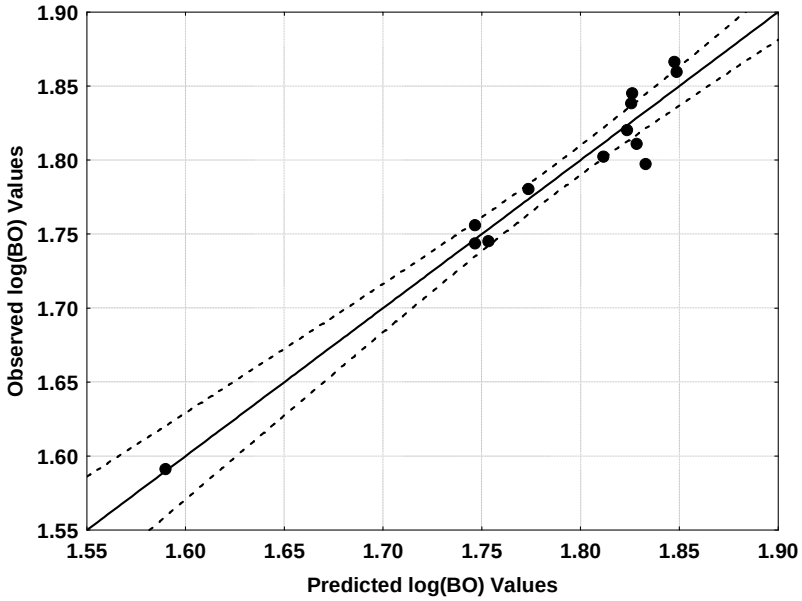

Figure 3: Plot of observed versus predicted values (Eq. 2) of log(BO). Dashed lines denote the 95% confidence interval.

Results for the *in vitro* antimalarial activity against the D6 strain.

For the antimalarial activity against the D6 strain we obtained the following statistically significant equation:

$$\log(IC_{50}) = 0.36 - 4.33S_{13}^N(LUMO+1)^* - 22.53F_{28}(LUMO+1)^* \quad (3)$$

with n=13, R=0.97, R^2=0.94, adj R^2=0.92, F(2,9)=67.20 (*p<0.000001*) and SD=0.19. No outliers were detected and no residuals fall outside the ±2σ limits. Here $S_{13}^N(LUMO+1)^*$ is the orbital nucleophilic superdelocalizability of the second vacant local MO localized on atom 13 and $F_{28}(LUMO+1)^*$ is the Fukui index of the second vacant local MO localized on atom 28. Table 6 shows the beta coefficients and the results of the t-test for significance of coefficients for the variables appearing in Eq. 2. Concerning independent variables, $r^2(S_{13}^N(LUMO+1)^*, F_{28}(LUMO+1)^*)$=0.18 shows that there is no significant internal correlation. Figure 4 shows the plot of observed *vs.* calculated values. The associated statistical parameters of Eq. 3 show that this equation is statistically significant and that the variation of a group of local atomic reactivity indices belonging to the common skeleton explains about 92% of the variation of the antimalarial activity against the D6 strain.

Table 6: Beta coefficients and *t*-test for significance of the coefficients in Eq. 3.

	Beta	t(9)	*p-level*
$S_{13}^N(LUMO+1)^*$	-1.06	-11.54	<0.00001
$F_{28}(LUMO+1)^*$	-0.36	-3.90	<0.004

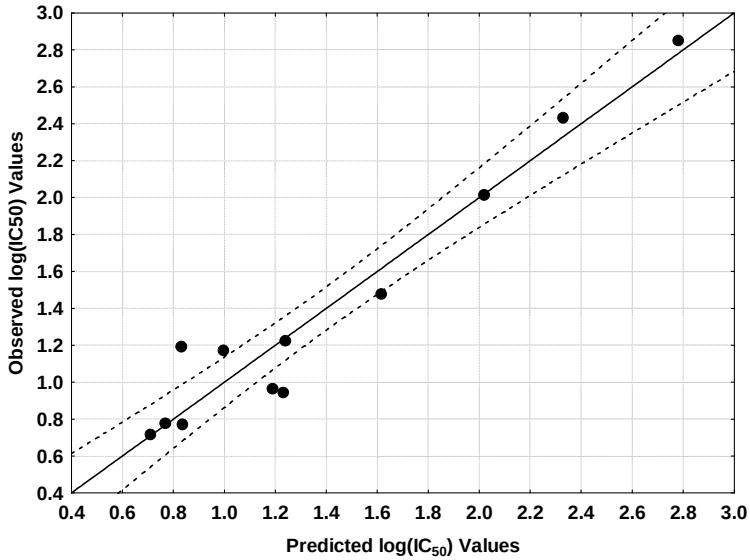

Figure 4: Plot of observed versus predicted values (Eq. 4) of log(IC_{50}). Dashed lines denote the 95% confidence interval.

Results for the *in vitro* antimalarial activity against the W2 strain.

For the antimalarial activity against the W2 strain we obtained the following statistically significant equation:

$$\log(IC_{50}) = -0.38 - 6.01 S_{13}^{N}(LUMO+1)^{*} - 40.72 F_{28}(LUMO+1)^{*} + 17.17 F_{22}(LUMO+1)^{*} \quad (4)$$

with n=13, R=0.98, R^2=0.96, adj R^2=0.95, F(3,8)=64.20 (*p<0.00001*) and SD=0.23. No outliers were detected and no residuals fall outside the ±2σ limits. Here $F_{22}(LUMO+1)^{*}$ is the Fukui index of the second vacant local MO localized on atom 22. The other two local atomic reactivity indices have the same meaning than in Eq. 3. Tables 7 and 8 show, respectively, the beta coefficients, the results of the t-test for significance of coefficients and the matrix of squared correlation coefficients for the variables appearing in Eq. 4. Table 8 shows that there are no significant internal correlations. Figure 5 shows the plot of observed *vs.* calculated values. The associated statistical parameters of Eq. 4 show that this equation is statistically significant and that the variation of a group of local atomic reactivity indices belonging to the common skeleton explains about 95% of the variation of the antimalarial activity against the W2 strain.

Table 7: Beta coefficients and *t*-test for significance of the coefficients in Eq. 4.

	Beta	t(8)	*p-level*
$S_{13}^{N}(LUMO+1)^{*}$	-1.03	-13.22	<0.000001
$F_{28}(LUMO+1)^{*}$	-0.45	-5.83	<0.0004
$F_{22}(LUMO+1)^{*}$	0.24	3.40	<0.009

Table 8: Squared correlation coefficients for the variables appearing in Eq. 4.

	$S_{13}^{N}(LUMO+1)^{*}$	$F_{28}(LUMO+1)^{*}$
$F_{28}(LUMO+1)^{*}$	0.18	1.00
$F_{22}(LUMO+1)^{*}$	0.004	0.0004

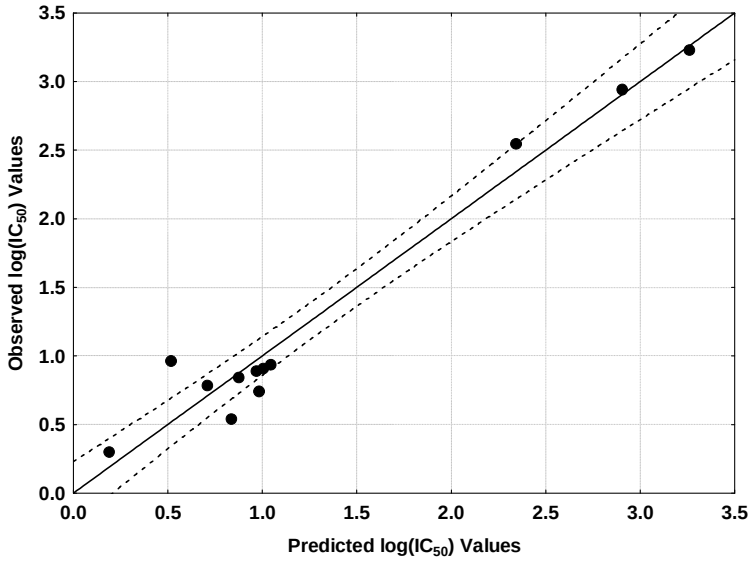

Figure 5: Plot of observed versus predicted values (Eq. 4) of log(IC_{50}). Dashed lines denote the 95% confidence interval.

Results for the *in vitro* antimalarial activity against the C235 strain.
For the antimalarial activity against the C235 strain we obtained the following statistically significant equation:

$$\log(IC_{50}) = -2.07 - 2.72S_{13}^{N}(LUMO+1)^{*} - 5.84Q_{24} \quad (5)$$

with n=13, R=0.96, R^2=0.93, adj R^2=0.91, F(2,9)=59.87 (*p<0.00001*) and SD=0.24. No outliers were detected and no residuals fall outside the ±2σ limits. Here Q_{24} is the net charge of atom 24. Table 6 shows the beta coefficients and the results of the t-test for significance of coefficients for the variables appearing in Eq. 5. On the subject of independent variables, $r^2(S_{13}^{N}(LUMO+1)^{*}, Q_{24})$=0.17 shows that there is no significant internal correlation. Figure 6 shows the plot of observed *vs.* calculated values. The associated statistical parameters of Eq. 5 show that this equation is statistically significant and that the variation of a group of local atomic reactivity indices belonging to the common skeleton explains about 91% of the variation of the antimalarial activity against the C235 strain.

Table 9: Beta coefficients and *t*-test for significance of the coefficients in Eq. 5.

	Beta	t(9)	*p-level*
$S_{13}^{N}(LUMO+1)^{*}$	-0.57	-4.95	<0.0008
Q_{24}	-0.50	-4.31	<0.002

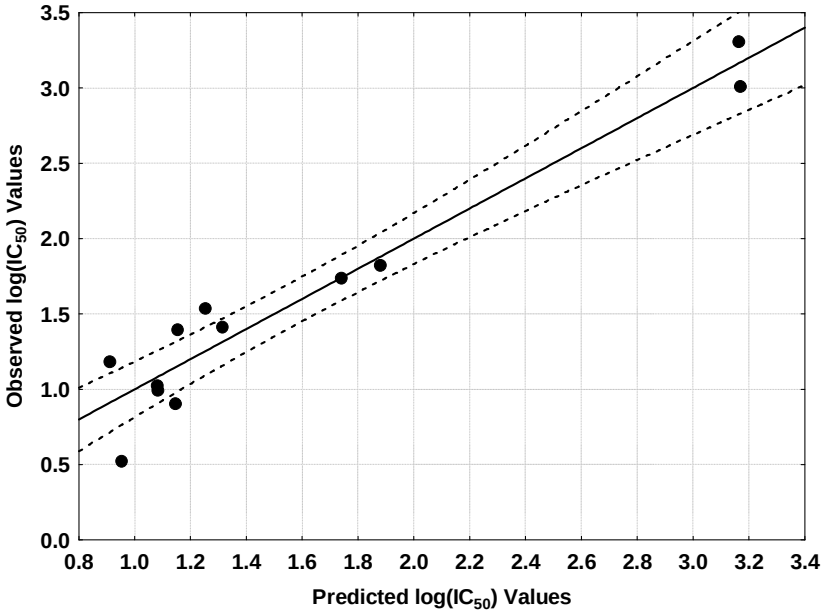

Figure 6: Plot of observed versus predicted values (Eq. 5) of log(IC_{50}). Dashed lines denote the 95% confidence interval.

No statistically significant equation was obtained for the relationship between electronic structure and cytotoxicity.

DISCUSSION

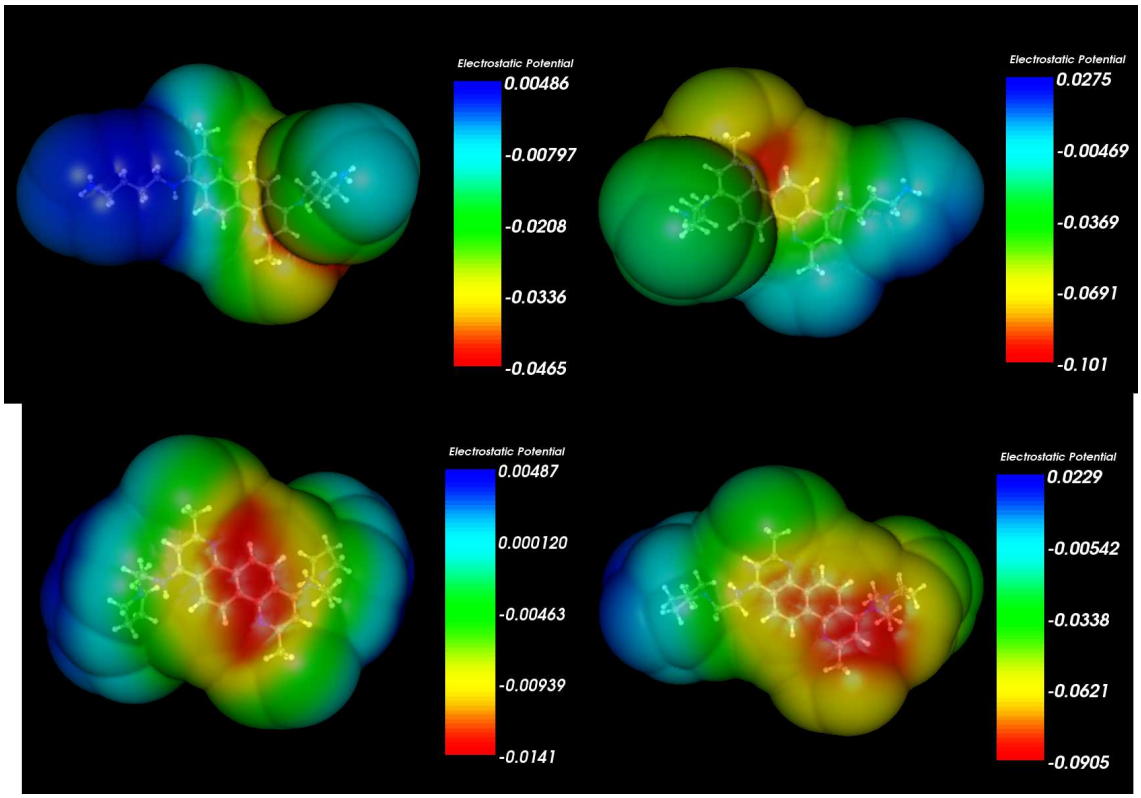

Figure 7. MEP of molecules 2 (upper left), 3 (upper right), 9 (lower left) and 11 (lower right) at 3.5 Å of the nuclei.

Conformational aspects and Molecular Electrostatic Potential

Several side chains of the systems studied here have a large enough degree of conformational freedom to allow a suggestion of what their orientation could be at the moment of the interaction that produces their biological action. To get an idea about what local minima exist, a study should be made starting from the fully optimized geometry and exploring only the surface available up to 7 kcal/mole [26]. Nevertheless, as we shall see below, some results

allow us to impose some conformational restrictions on the side chains. Some examples of the influence of the position of the side chains on the structure of the Molecular Electrostatic Potential (MEP) are shown in Figure 7.

We can see that the MEPs are enough different to allow a suggestion of what conformation might be adopted in the earlier stages of the recognition and guiding process.

BoNT/A LC Inhibition.

Table 4 indicates that the importance of the variables is $F_{15}(LUMO+2)^*$ > $S_4^N(LUMO+1)^*$ > $S_{16}^E(HOMO-2)^*$. A Variable-by-Variable (VbV) analysis of Eq. 2 indicates that a high BoNT/A LC percentage of inhibition is associated with a low value of $F_{15}(LUMO+2)^*$ and with high values of $S_{16}^E(HOMO-2)^*$ and $S_4^N(LUMO+1)^*$. A low value of $F_{15}(LUMO+2)^*$ can be obtained only by lowering its electron population. If we consider that $F_{15}(LUMO)^*$, $F_{15}(LUMO+1)^*$ and $F_{15}(LUMO+2)^*$ are of π nature, a consistent interpretation if that atom 15 is interacting with an electron-rich center through $F_{15}(LUMO)^*$ and $F_{15}(LUMO+1)^*$, while $F_{15}(LUMO+2)^*$ seems to hinder the interaction through a repulsive interaction with σ MOs located on the partner. It is worth remembering that $F_{15}(LUMO)^*$ and $F_{15}(LUMO+1)^*$ do not appear in Eq. 2 because their variation is not statistically significant (i.e., they are constants). A high value of $S_{16}^E(HOMO-2)^*$ indicates that atom 16 is interacting with an electron-deficient center through its two highest local occupied MOs. A high value of $S_4^N(LUMO+1)^*$, a π MO, suggests that atom 4 is interacting with an electron-rich center through its two lowest vacant MOs. The corresponding two-dimensional (2D) partial pharmacophore is shown in Fig. 8.

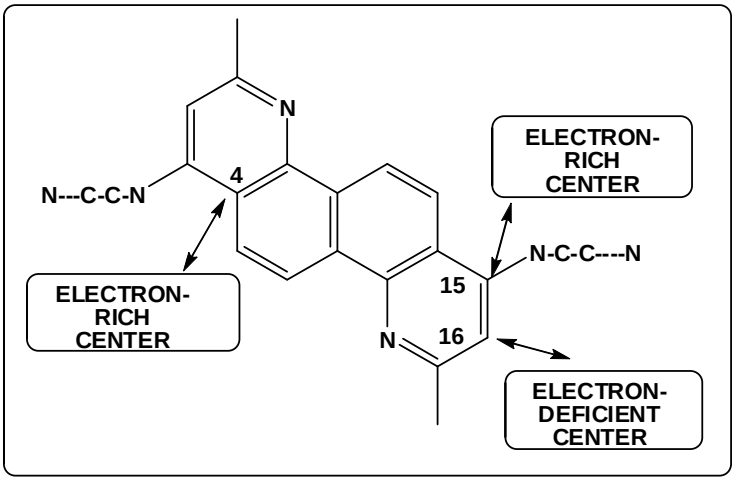

Figure 8. Partial 2D pharmacophore for the BoNT/A LC inhibition percentage.

These results clearly show that the aromatic system is involved in the inhibitory process. Moreover, considering that atom 15 is interacting with an electron-rich center while its neighbor atom 16 interacts with an electron-deficient center, part of or the entire ring to which they belong might be interacting with an aromatic moiety through π-π stacking. Regarding the side chains, our results do not allow us to make any definitive statement about their role. Nevertheless, our local atomic reactivity indices may help in the following way. Burnett, Bavari et al. suggested that an "unfavorable hydrophobic-polar or polar-polar contact between one (or both) of the morpholine rings (12 and 13 in Table 2) and an enzyme residue(s) is occurring in the BoNT/A LC binding site" [2]. This hypothesis is sustained by the fact that molecule 10, which has a ring composed only of saturated carbon atoms, is more potent. Figure 9 shows the local atomic hardnesses of the piperidine and morpholine substituents of molecules 10 and 12.

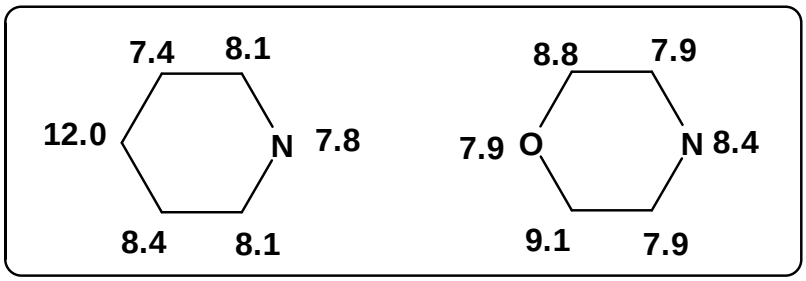

Figure 9. Local atomic hardnesses (eV) of the atoms of the end substituents of side chains in molecules 10 (left) and 12 (right).

We can see that the four carbon atoms of the morpholine substituent have about equal or greater hardness than their piperidine equivalents. Nevertheless, in the morpholine substituent the oxygen atom has a noticeably lesser hardness (7.9 eV) that its carbon atom equivalent (12 eV) in the piperidine substituent. Therefore we may state confidently that the piperidine substituent is more prone to interact with apolar sites than morpholine. A more likely hypothesis is that the lone pairs of the oxygen atom on the morpholine substituent are the cause of the lowering of activity. Figure 10 shows the MEP map of the piperidine substituent of molecule 10 (left) and the morpholine substituent of molecule 12 (right).

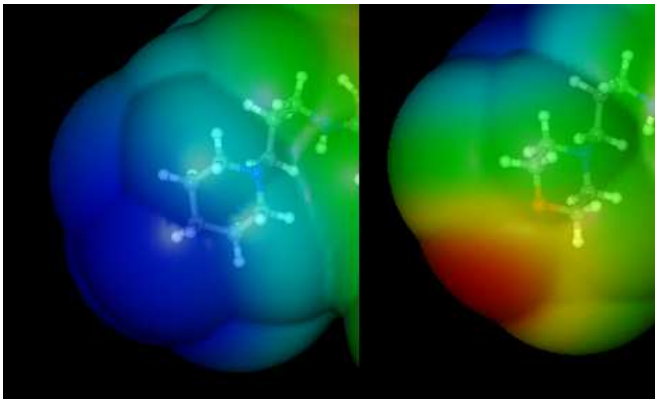

Figure 10. MEP map of the piperidine substituent of molecule 10 (left) and the morpholine substituent of molecule 12 (right).

We can see that the MEP of the piperidine group has a positive area (in blue) around its end while in the equivalent area in the morpholine group the MEP is negative (in red and yellow). This is a direct effect of the lone pairs of the oxygen atom. As molecule 12 is active and we have a distribution of side chain conformations close to the active site, it is possible that only a few present a positive MEP area pointing to the active site. Then the methylene group located at the end of the piperidine substituent is a good target to investigate (by substituting a H atom by alkyl groups). This is also indirect evidence that one or both side chains participate in the inhibitory process.

***In vitro* antimalarial activity.**

It was suggested that these molecules act by blocking the formation of β-hematin, like 4-amino-7-chloroquinoline-based antimalarial compounds [2]. This causes an increase of toxic heme within the parasite's food vacuole and its subsequent death. We may appreciate that Eqs. 3, 4 and 5 have $S_{13}^{N}(LUMO+1)^*$ as a common component and that Eqs. 3 and 4 have also $F_{28}(LUMO+1)^*$ as a common component. Given the high correlation between the experimental data (see Table 3) we shall work within the hypothesis that the inhibitory mechanism is the same for all three malaria strains. This guess is supported by the facts that, for good antimalarial activity, the requirement of a low value of $S_{13}^{N}(LUMO+1)^*$ holds for Eqs. 3 to 5 and the condition for a high value of $F_{28}(LUMO+1)^*$ holds for Eqs. 3 and 4. These requirements indicate that atom 13 interacts with an electron-rich center through its local LUMO* and that atom 28 also interacts with an electron-rich center through its two lowest local vacant MOs. Given the position of atom 13 within the molecule, it is highly probable that it interacts through π-π stacking. Atom 28 is the nitrogen atom located at the end of one of the chains (see Fig. 2). As Fig. 11 shows, the two lowest local vacant MOs of atom 28 are of σ nature (maybe with an n component).

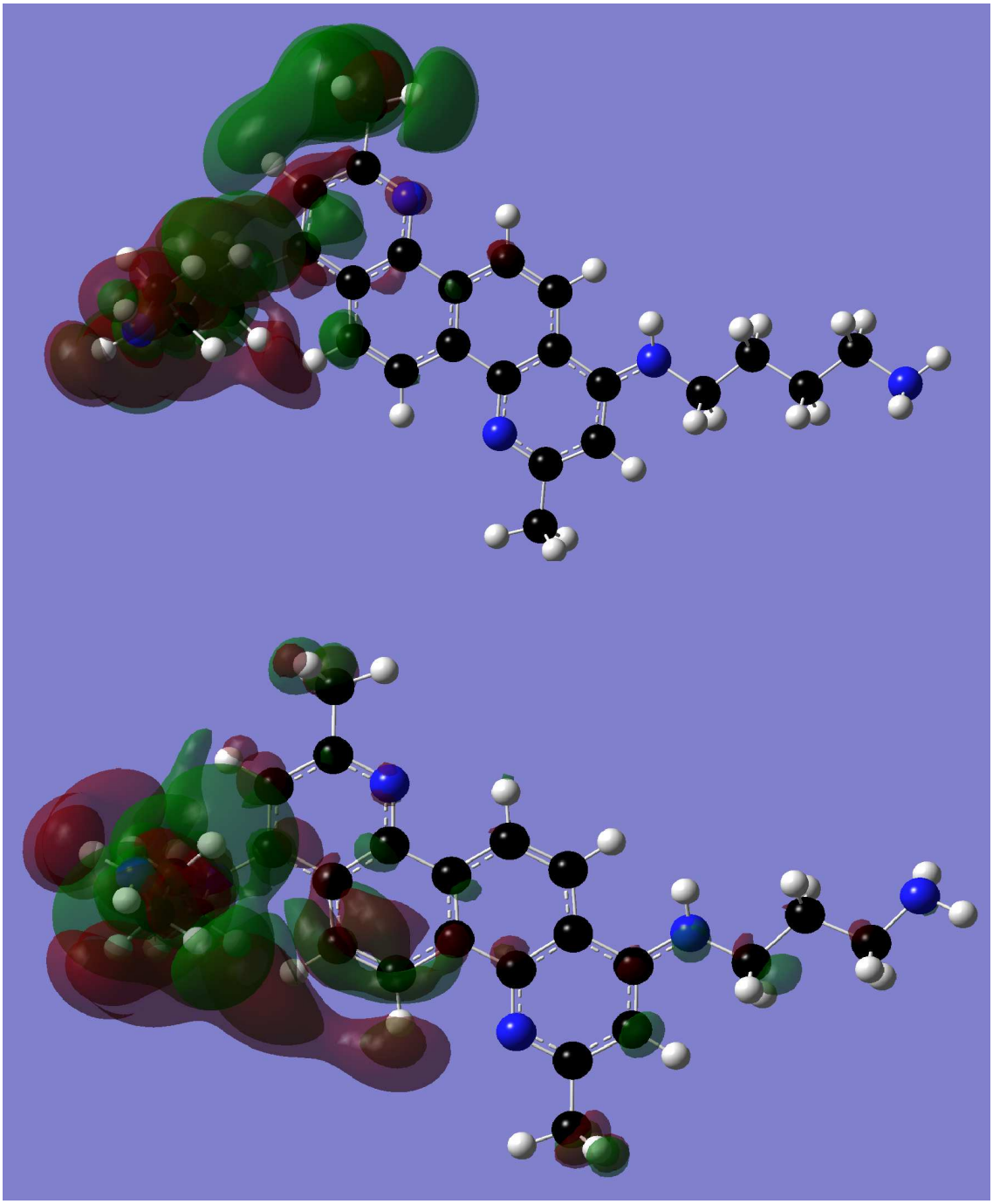

Figure 11. The two lowest vacant local MOs of molecules 2 (upper) and 3 (lower). Atom 28 is located at the far left of the figures.

A low value for $F_{22}(LUMO+1)^*$ is associated with high antimalarial activity. Atom 22 is a carbon atom belonging to the other side chain (See Fig. 2). For this case we suggest that atom 22 lies close to an electron-rich center of its partner. Atom 24 is the nitrogen atom belonging to the same side chain as atom 22 (Fig. 2) and usually has a negative net charge. As a positive net charge on atom 24 is required for good antimalarial activity, the ideal situation would be that the N atom should have the lowest possible negative charge. For example, in the morpholine substituent of molecules 12 and 13 atom 24 has a diminished negative net charge. Therefore atom 24 could be a possible target for modifications leading to enhanced antimalarial activity. Figure 12 shows the corresponding partial 2D pharmacophore for antimalarial activity. Finally, the nature of the suggested electron-rich areas interacting with the side chains cannot be elucidated for the moment.

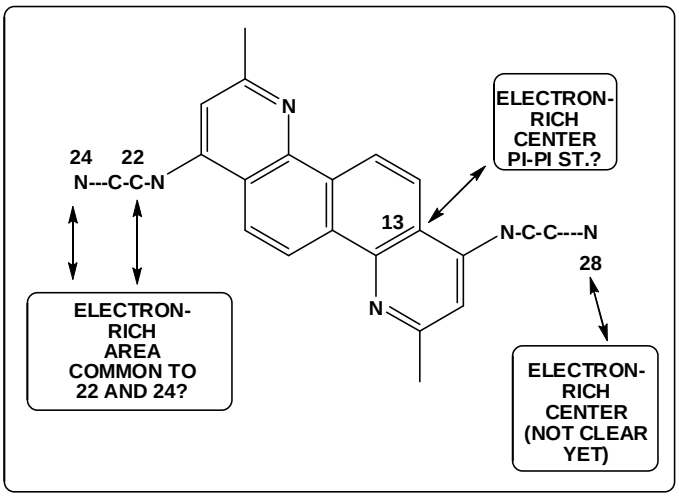

Figure 12. Partial 2D pharmacophore for antimalarial activity.

From these results it seems highly likely that the aromatic ring and both side chains are essential for antimalarial activity in this kind of compounds. Besides the possible modifications to atom 28 to reduce its negative net charge, another point to explore by medicinal chemists is the detection of the optimal length and the active conformation (or conformations) of the side chains. Note the important fact that we have assumed that the terminal N atom of the side chains is equivalent in all molecules despite the differences in the length of the side chain. Finally, note that the variation of all biological activities studied here is orbital-controlled [59].

CONCLUSION

We obtained good statistically significant relationships relating electronic structure with the percentage of BoNT/A LC inhibition and the antimalarial activity for a group of 1,7-bis-(aminoalkyl)diazachrysene derivatives. For the BoNT/A LC percentage of inhibition there is indirect evidence supporting the interaction of one or both side chains with the site. In the case of antimalarial activity both side chains seem to participate in the inhibitory process. The biological activities are highly orbital-controlled, as a result of the long evolutionary process of living beings. We suggest some atomic targets to improve the antimalarial activity.

Acknowledgements
Prof. Dr. Bruce K. Cassels (Faculty of Sciences, University of Chile) is thanked for helpful comments.

REFERENCES

[1] RS Rapaka; A Makriyannis, *Structure-activity relationships of the cannabinoids*, U.S. Dept. of Health and Human Services, Public Health Service, Alcohol, Drug Abuse, and Mental Health Administration, Rockville, MD., Washington, D.C., **1987**.
[2] I Opsenica; JC Burnett; R Gussio; D Opsenica; N Todorović, et al., *J. Med. Chem.*, **2011**, 54, 1157-1169.
[3] C Rasetti-Escargueil; S Surman-Lee, *Clostridium botulinum: a spore forming organism and a challenge to food safety*, Nova Science Publishers, New York, **2012**.
[4] M Bungay Stanier, *End malaria: bold innovation, limitless generosity, and the opportunity to save a life*, Do You Zoom, Inc., Dobbs Ferry, NY., **2011**.
[5] K-c Yip, *Disease, colonialism, and the state: Malaria in modern East Asian history*, Hong Kong University Press, Hong Kong, **2009**.
[6] JLA Webb, *Humanity's burden: a global history of malaria*, Cambridge University Press, Cambridge, **2009**.
[7] T Awash; UN Millennium Project. Working Group on Malaria., *Coming to grips with malaria in the new millennium*, Earthscan, London; Sterling, Va., **2005**.
[8] M Rosaler, *Botulism*, Rosen Pub. Group, New York, **2004**.
[9] AJ Bollet, *Plagues & poxes: the impact of human history on epidemic disease*, Demos, New York, **2004**.
[10] D Armus, *Disease in the history of modern Latin America: from malaria to AIDS*, Duke University Press, Durham N.C., **2003**.
[11] R Sallares, *Malaria and Rome: a history of malaria in ancient Italy*, Oxford University Press, Oxford, **2002**.
[12] J Dickie; J Foot; FM Snowden, *Disastro!: disasters in Italy since 1860: culture, politics, society*, Palgrave, New York, **2002**.

[13] C Montecucco, *Clostridial neurotoxins: the molecular pathogenesis of tetanus and botulism*, Springer, Berlin; London, **1995**.
[14] G Harrison, *Mosquitoes, malaria and man: a history of the hostilities since 1880*, J. Murray, London, **1978**.
[15] A Celli; A Celli-Fraentzel, *The history of malaria in the Roman Campagna from ancient times*, Bale & Danielsson, London,, **1933**.
[16] GR Leighton, *Botulism and food preservation (The Loch Maree tragedy)*, W. Collins Sons & Co., London, **1923**.
[17] WHS Jones; ET Withington, *Malaria and Greek history*, Manchester University Press, Manchester, **1909**.
[18] WHS Jones; R Ross; GG Ellet, *Malaria: a neglected factor in the history of Greece and Rome*, Bowes & Bowes, Cambridge, **1907**.
[19] JS Gómez Jeria, *Boll. Chim. Farmac.*, **1982**, 121, 619-625.
[20] JS Gómez-Jeria, *Int. J. Quant. Chem.*, **1983**, 23, 1969-1972.
[21] JS Gómez-Jeria; D Morales-Lagos, "The mode of binding of phenylalkylamines to the Serotonergic Receptor," in *QSAR in design of Bioactive Drugs*, M. Kuchar Ed., pp. 145-173, Prous, J.R., Barcelona, Spain, **1984**.
[22] JS Gómez-Jeria; DR Morales-Lagos, *J. Pharm. Sci.*, **1984**, 73, 1725-1728.
[23] JS Gómez-Jeria; D Morales-Lagos; JI Rodriguez-Gatica; JC Saavedra-Aguilar, *Int. J. Quant. Chem.*, **1985**, 28, 421-428.
[24] JS Gómez-Jeria; D Morales-Lagos; BK Cassels; JC Saavedra-Aguilar, *Quant. Struct.-Relat.*, **1986**, 5, 153-157.
[25] JS Gómez-Jeria; P Sotomayor, *J. Mol. Struct. (Theochem)*, **1988**, 166, 493-498.
[26] JS Gómez-Jeria, "Modeling the Drug-Receptor Interaction in Quantum Pharmacology," in *Molecules in Physics, Chemistry, and Biology*, J. Maruani Ed., vol. 4, pp. 215-231, Springer Netherlands, **1989**.
[27] JS Gómez-Jeria; M Ojeda-Vergara; C Donoso-Espinoza, *Mol. Engn.*, **1995**, 5, 391-401.
[28] JS Gómez-Jeria; L Lagos-Arancibia, *Int. J. Quant. Chem.*, **1999**, 71, 505-511.
[29] JS Gómez-Jeria; L Lagos-Arancibia; E Sobarzo-Sánchez, *Bol. Soc. Chil. Quím.*, **2003**, 48, 61-66.
[30] JS Gómez-Jeria; M Ojeda-Vergara, *J. Chil. Chem. Soc.*, **2003**, 48, 119-124.
[31] JS Gómez-Jeria; F Soto-Morales; G Larenas-Gutierrez, *Ir. Int. J. Sci.*, **2003**, 4, 151-164.
[32] JS Gómez-Jeria; LA Gerli-Candia; SM Hurtado, *J. Chil. Chem. Soc.*, **2004**, 49, 307-312.
[33] F Soto-Morales; JS Gómez-Jeria, *J. Chil. Chem. Soc.*, **2007**, 52, 1214-1219.
[34] JS Gómez-Jeria; F Soto-Morales; J Rivas; A Sotomayor, *J. Chil. Chem. Soc.*, **2008**, 53, 1393-1399.
[35] JS Gómez-Jeria, *J. Chil. Chem. Soc.*, **2010**, 55, 381-384.
[36] C Barahona-Urbina; S Nuñez-Gonzalez; JS Gómez-Jeria, *J. Chil. Chem. Soc.*, **2012**, 57, 1497-1503.
[37] T Bruna-Larenas; JS Gómez-Jeria, *Int. J. Med. Chem.*, **2012**, 2012 Article ID 682495, 1-16.
[38] DA Alarcón; F Gatica-Díaz; JS Gómez-Jeria, *J. Chil. Chem. Soc.*, **2013**, 58, 1651-1659.
[39] JS Gómez-Jeria, *Elements of Molecular Electronic Pharmacology (in Spanish)*, Ediciones Sokar, Santiago de Chile, **2013**.
[40] JS Gómez-Jeria, *Canad. Chem. Trans.*, **2013**, 1, 25-55.
[41] JS Gómez-Jeria; M Flores-Catalán, *Canad. Chem. Trans.*, **2013**, 1, 215-237.
[42] A Paz de la Vega; DA Alarcón; JS Gómez-Jeria, *J. Chil. Chem. Soc.*, **2013**, 58, 1842-1851.
[43] I Reyes-Díaz; JS Gómez-Jeria, *J. Comput. Methods Drug Des.*, **2013**, 3, 11-21.
[44] JS Gómez-Jeria, *Int. Res. J. Pure App. Chem.*, **2014**, 4, 270-291.
[45] JS Gómez-Jeria, *Der Pharm. Lett.*, **2014**, 6., 95-104.
[46] JS Gómez-Jeria, *Brit. Microbiol. Res. J.*, **2014**, In press.,
[47] JS Gómez-Jeria, *SOP Trans. Phys. Chem.*, **2014**, In press,
[48] D Muñoz-Gacitúa; JS Gómez-Jeria, *J. Comput. Methods Drug Des.*, **2014**, 4, 33-47.
[49] D Muñoz-Gacitúa; JS Gómez-Jeria, *J. Comput. Methods Drug Des.*, **2014**, 4, 48-63.
[50] DI Pino-Ramírez; JS Gómez-Jeria, *Amer. Chem. Sci. J.*, **2014**, 4, 554-575.
[51] F Salgado-Valdés; JS Gómez-Jeria, *J. Quant. Chem.*, **2014**, 2014 Article ID 431432, 1-15.
[52] R Solís-Gutiérrez; JS Gómez-Jeria, *Res. J. Pharmac. Biol. Chem. Sci.*, **2014**, 5, 1401-1416.
[53] RS Mulliken, *J. Chem. Phys.*, **1955**, 23, 1833-1840.
[54] K Fukui; H Fujimoto, *Frontier orbitals and reaction paths: selected papers of Kenichi Fukui*, World Scientific, Singapore; River Edge, N.J., **1997**.
[55] MJ Frisch; GW Trucks; HB Schlegel; GE Scuseria; MA Robb, et al., Gaussian98 Rev. A.11.3, Gaussian, Pittsburgh, PA, USA, **2002**.
[56] JS Gómez-Jeria, D-Cent-QSAR: A program to generate Local Atomic Reactivity Indices from Gaussian log files. v. 1.0, Santiago, Chile, **2014**.
[57] JS Gómez-Jeria, *J. Chil. Chem. Soc.*, **2009**, 54, 482-485.
[58] Statsoft, Statistica 8.0, 2300 East 14 th St. Tulsa, OK 74104, USA, **1984-2007**.
[59] G Klopman, *J. Am. Chem. Soc.*, **1968**, 90, 223-234.